Electrochemical attosyringe

François O. Laforge, James Carpino, Susan A. Rotenberg, and Michael V. Mirkin*

Department of Chemistry and Biochemistry, Queens College–City University of New York, Flushing, NY 11367

Communicated by Allen J. Bard, University of Texas, Austin, TX, June 1, 2007 (received for review April 5, 2007)

The ability to manipulate ultrasmall volumes of liquids is essential in such diverse fields as cell biology, microfluidics, capillary chromatography, and nanolithography. In cell biology, it is often necessary to inject material of high molecular weight (e.g., DNA, proteins) into living cells because their membranes are impermeable to such molecules. All techniques currently used for microinjection are plagued by two common problems: the relatively large injector size and volume of injected fluid, and poor control of the amount of injected material. Here we demonstrate the possibility of electrochemical control of the fluid motion that allows one to sample and dispense attoliter-to-picoliter (10^{-18} to 10^{-12} liter) volumes of either aqueous or nonaqueous solutions. By changing the voltage applied across the liquid/liquid interface, one can produce a sufficient force to draw solution inside a nanopipette and then inject it into an immobilized biological cell. A high success rate was achieved in injections of fluorescent dyes into cultured human breast cells. The injection of femtoliter-range volumes can be monitored by video microscopy, and current/resistance-based approaches can be used to control injections from very small pipettes. Other potential applications of the electrochemical syringe include fluid dispensing in nanolithography and pumping in microfluidic systems.

liquid/liquid interface | microinjection | nanopipette | fluid delivery | nanopump

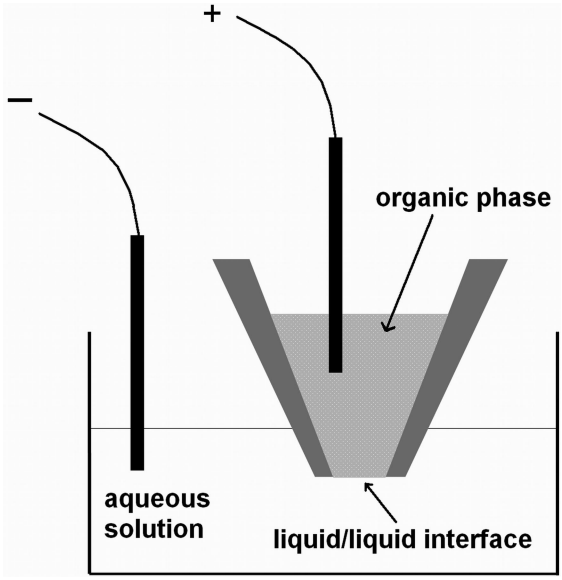

Fig. 1. Scheme of the electrochemical attosyringe.

Many biologically important molecules, such as DNA and proteins, cannot cross the cell membrane. Microinjection techniques are widely used in cell biology when one needs to introduce such substances into the cytoplasm of living cells (1). Important advantages of microinjection over other techniques, such as lipofection (2) and electroporation (3), include the abilities to target specific cells and inject practically any material into the cell with some degree of spatial selectivity (4).

The most common mode of microinjection is "stab injection," where a micropipette rapidly perforates the cell membrane, injects some amount of material, and withdraws. However, it is difficult to control either the location of the pipette tip during the stab injection or the amount of the injected material (5). These problems, along with a relatively large pipette tip size (usually micrometers) and high volume of the injected solution, often cause damage to cells and dramatically decrease the injection success rate (6). The above limitations, which are common to pressure microinjectors, are largely due to the difficulty in using high pressures to move liquid through a submicrometer-sized pipette orifice. Some novel approaches were used recently to overcome this problem. For example, Knoblauch *et al.* (6) introduced an injector based on the temperature expansion of a liquid alloy. However, controlling the amount of heat delivered to the alloy during the injection and the dispensed volume may not be straightforward, especially in the case of multiple injections. Among other recently reported devices are an electroosmosis-based nanopipettor that can deliver picoliter-range volumes (7), a cell nanoinjector, in which cargo is delivered by a carbon nanotube used as an atomic force microscopy tip (8), and a double-barrel nanopipette for depositing liquid drops on a surface (9).

Here, we describe a unique device for cellular injections: an "electrochemical attosyringe." The device consists of a nanopipette that is produced by heat-pulling a capillary and separating it into two halves, each of which is shaped as a needle. The radius of the pipette orifice depends of the choice of pulling parameters and can be varied from a few nanometers to >1 μm. The prepared nanopipette is filled with a water-immiscible organic solvent and immersed in an aqueous solution (Fig. 1). The potential drop between the two liquid phases can be controlled by applying voltage between the reference electrode inserted in the pipette and another reference electrode immersed in the outer solution. It is well known that the application of voltage across the liquid/liquid interface changes the surface tension (10). We discovered recently that the resulting force is sufficiently strong to induce the flow of liquid into/out of the pipette. When the potential of the inner (organic) solution is made negative, the shape of the meniscus at the interface of the two liquids changes, and water enters the pipette. The application of a sufficiently positive potential to the inner reference electrode results in the expulsion of water. Here we make use of this effect to deliver ultrasmall volumes of solution into mammalian cells in culture.

Results

Sampling and Dispensing Fluids with the Attosyringe. The potential control of the fluid injection/ejection is shown in Fig. 2. The images

Author contributions: F.O.L. and M.V.M. designed research; F.O.L. performed research; J.C. and S.A.R. contributed new reagents/analytic tools; M.V.M. analyzed data; and F.O.L. and M.V.M. wrote the paper.

The authors declare no conflict of interest.

Abbreviations: DCE, 1,2-dichloroethane; EB, ethidium bromide; SECM, scanning electrochemical microscope.

*To whom correspondence should be addressed. E-mail: michael.mirkin@qc.cuny.edu.

This article contains supporting information online at www.pnas.org/cgi/content/full/0705102104/DC1.

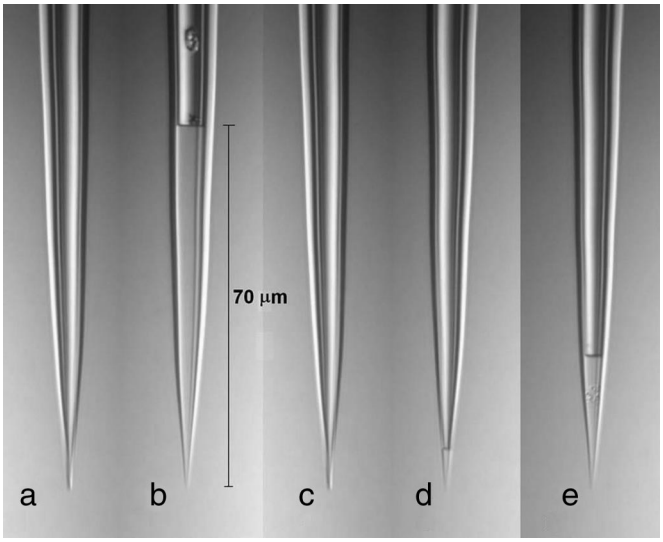

Fig. 2. Sequential ingress/egress of water in a DCE-filled nanopipette. (*a*) Initial immersion, $E = +600$ mV. (*b*) Ingress of water after the voltage was stepped to -100 mV an then to $+90$ mV. (*c*) Complete egress of water at $E = +600$ mV. (*d*) Same as *b*, but with a shorter step time at $E = -100$ mV. (*e*) The voltage was stepped again to -100 mV and then back to $+90$ mV. The aperture radius was ≈300 nm. The pipette was filled with 10 mM THATPBCl in DCE and immersed in 10 mM KF aqueous solution.

in Fig. 2 were obtained with a video microscope (approximately × 1,000) focused on the tip of a nanopipette filled with 1,2-dichloroethane (DCE) solution. In Fig. 2*a*, the interfacial voltage (E) was maintained at +600 mV (organic phase positive) to prevent the ingress of water inside the pipette. When the voltage was lowered to -100 mV, the aqueous solution immediately flowed inside the pipette. This flow was stopped by stepping the organic phase potential to approximately +90 mV (Fig. 2*b*). The volume of aqueous solution inside the pipette remained constant as long as the potential was held at +90 mV. When the potential was stepped back to approximately +600 mV, aqueous solution was completely removed from the pipette (Fig. 2*c*). This injection/ejection process could be performed repeatedly with the same nanopipette, as shown in Fig. 2 *d* and *e*.

In a very similar way, one can fill the pipette with water and immerse it in a water-immiscible liquid (e.g., organic solvent). This arrangement, which enables the injection/ejection of liquids other than water, is potentially useful, e.g., for nanolithography and sample injection in capillary electrophoresis and automated analysis systems. Details of these experiments are available in supporting information (SI) *Text* and SI Fig. 8.

The volume of injected solution depends strongly on the pipette radius, the duration of the potential step, and its amplitude. For the sake of visibility, the nanopipette used in Fig. 2 was relatively large (aperture radius, $a \cong 300$ nm). In Fig. 2 *b*, *d*, and *e*, a long, a short, and an intermediate time step were used, thus showing different volumes of solution sampled inside the pipette. Assuming that the pipette tip approximates a truncated cone geometry, one can evaluate these volumes as 2,300, 500, and 23 fl, respectively (1 fl = 1 $\mu m^3 = 10^{-15}$ liter). The smallest volume that can be dispensed with such a pipette is ≈1 fl. However, much smaller pipettes (i.e., $a < 10$ nm) can easily be produced (11) and used to dispense as little as <1 al (i.e., 10^{-18} liter) of liquid. Estimating the solution volume is straightforward when it is relatively large (e.g., >1 fl). Smaller volumes can be evaluated and injections from very small pipettes can be monitored by measuring the pipette resistance and/or current vs. potential curves.

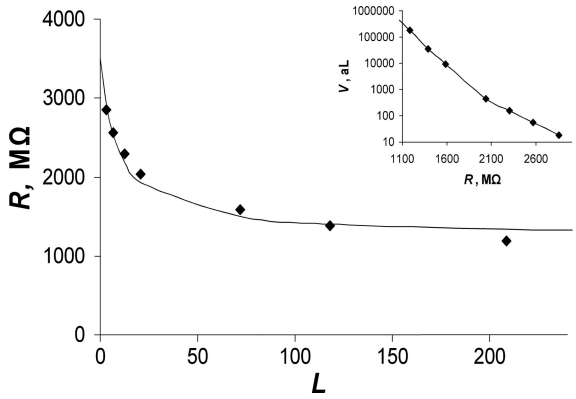

Fig. 3. Dependence of the pipette resistance on the amount of water drawn into it. Measured values of pipette resistance (symbols) are fitted to the theory (solid line). The best fit was obtained with $R_{out} = 1.2$ GΩ. The pipette was filled with DCE containing 10 mM THATPBCl and immersed in a 100 mM $MgSO_4$ aqueous solution. $a = 110$ nm, $\alpha = 6.3°$, $\kappa_{inner} = 114$ μS/cm, and $\rho^{outer}_{inner} = 56$. (*Inset*) The correspondent volume vs. resistance dependence calculated from Eq. **2**.

Volume Control by Resistance Measurements. The organic phase conductivity usually is much lower than that of the aqueous solution. The total pipette resistance is largely determined by that of solution filling its narrow shaft. Thus, the ingress of the external liquid into the pipette produces either a significant increase (when organic solvent is drawn into the water-filled pipette) or decrease (when water is drawn into the organic-filled pipette) in pipette resistance, which can be used to evaluate the volume of the loaded solution. The inside of a laser-pulled micropipette has a shape of a truncated cone that can be described by two parameters: the pipette aperture radius, a, and the angle between the cone element and its axis, α. When the outer solution ingresses into the pipette up to a height h with respect to the orifice, the theoretical value of the pipette resistance can be obtained from Eq. **1**:

$$R = R_{out} + \frac{1}{\kappa_{inner} \pi a \tan \alpha} \left(\frac{\rho^{inner}_{outer}}{1 + [L \tan \alpha]^{-1}} + \frac{1}{1 + L \tan \alpha} \right), \quad [1]$$

where $\rho^{inner}_{outer} = \kappa_{inner}/\kappa_{outer}$ is the ratio of conductivity of the inner solution to that of the outer solution, $L = h/a$, and R_{out} includes the external solution resistance and the interfacial ion-transfer resistance (see *SI Appendix* for details).

Fig. 3 shows the fit between the theory (Eq. **1**; solid line) and the experimental data for a pipette radius $a = 110$ nm (symbols). One should notice that there is only one fitting parameter, R_{out}. All other quantities were determined independently, and their values were not used as adjustable parameters. The pipette radius was found from ion-transfer voltammetry using the second half of the same pipette (11). $\kappa_{inner} = 114$ μS/cm and $\rho^{inner}_{outer} = 56$ were determined by conductimetry. $\alpha = 6.3°$ was determined from optical micrographs of the pipette.

The volume of the second liquid phase inside the pipette can be calculated as follows (see *SI Appendix* for details)

$$V = \frac{\pi a^3}{3 \tan \alpha} ((1 + L \tan \alpha)^3 - 1). \quad [2]$$

Table 1 shows the V values obtained from Eq. **2** for different R and L values. The smallest measured volume of the filling solution in Table 1 is 18 al, and the smallest volume of dispensed

Table 1. Resistance (*R*), *L*, and volume (*V*) values obtained from Fig. 3

R, MΩ	*L*	*V*, al
1,339	208.6	175,270
1,406	117.9	34,738
1,497	72.0	9,029
1,928	20.9	443
2,193	12.5	158
2,536	6.8	55
2,923	3.1	18

liquid was 37 al. Smaller volumes can be evaluated by interpolating the R vs. L curve between $L = 0$ and the first point for experimental point and/or by using smaller pipettes.

Injection Control by Measuring Current–Voltage Curves. If a pipette is too small for video microscopic observation, the ingress/egress of the outer liquid can be monitored by recording current vs. voltage (or current vs. time) dependencies. The main goal here is to avoid the complete expulsion of water from the pipette, which may cause damage to the cell membrane if it comes into direct contact with organic filling solution. Fig. 4 shows a current vs. time curve (curve 2), which was obtained by changing the voltage applied to a 400-nm-radius pipette (curve 1). Curve 2 consists of several linear portions and two highly nonlinear regions occurring within the time interval between ≈30 and ≈45 s. Video micrographs obtained simultaneously with electrical measurements (not shown) showed that the linear current vs. time (or current vs. voltage) behavior was observed when the pipette was completely filled with DCE. This ohmic response could be fitted to the theory (dashed line) assuming the constant pipette resistance, $R = 550$ MΩ.

In contrast, highly nonlinear current–voltage response corresponds to changes in resistance caused by the ingress/egress of water. The ingress began at $t \cong 30$ s and ended at $t \cong 32$ s, when the current-time dependence became essentially linear again, but with a much steeper slope corresponding to a lower pipette resistance. Another region of nonlinear current–voltage behavior ($42 \text{ s} \leq t \leq 46$ s) corresponds to the expulsion of water from the pipette. When this process is complete, the current–time dependence becomes linear again and follows the same theoretical curve (dashed line). By stopping the injection after the current minimum but before the response becomes linear again, one can ensure that most, but not all, solution loaded into the pipette is ejected from it.

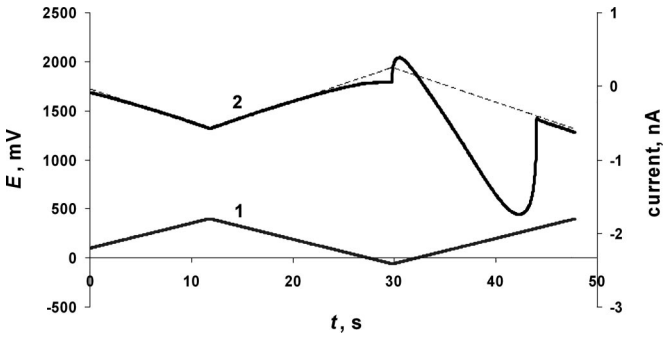

Fig. 4. Time dependences of the voltage applied to a pipette (1) and current flowing across the water/DCE interface (2) during the ingress and egress of the outer aqueous solution. The pipette was filled with DCE containing 10 mM THATPBCl and immersed in a 100 mM $MgSO_4$ solution. The pipette radius was 400 nm. The dashed line is the theoretical fit to the linear portions of the current response obtained with a pipette resistance, $R = 550$ MΩ.

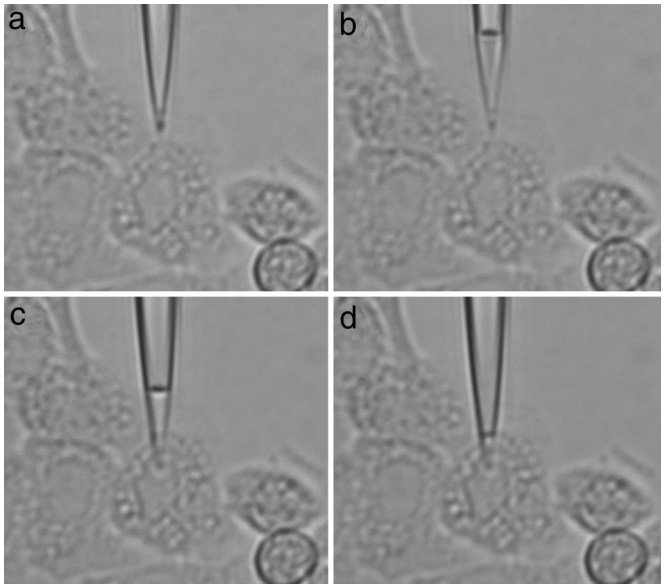

Fig. 5. Cell injection using the electrochemical syringe. (*a* and *b*) An ≈150-nm-radius pipette is positioned near the cell surface (*a*), and some amount of buffer solution is loaded into it (*b*). (*c*) The nanopipette is then translated toward the cell and penetrates the cell membrane. The buffer is injected inside the cell. (*d*) The injection was stopped before the organic solution reached the pipette tip.

Other modes of voltage control can also be used to operate the syringe, notably, an AC excitation or a cyclic voltage ramp. With a low-frequency AC voltage (up to ≈20 Hz; 200 mV amplitude) superimposed on a +90 mV DC bias, we observed liquid ingress and egress cycles at the same frequency, essentially synchronized with the applied AC voltage (see SI Movie 1). The electrochemical syringe operated in an AC mode can serve as nanopump driver for microfluidic applications.

Injection of Fluorescent Dye into Mammalian Cells. We used fluorescent dyes to investigate various aspects of attosyringe performance in cellular injections. The cultured human breast cells (MFC-10A) have been used in electrochemical experiments and showed excellent viability during >4-h time periods under similar experimental conditions (12). Two fluorescent dyes were used in our experiments, cationic ethidium bromide (EB) (13) and anionic BODIPY FLATP (14). It was shown previously that neither of them can cross a mammalian cell membrane.

The injection sequence is shown in Fig. 5. With the help of the scanning electrochemical microscope (SECM) (15), which was used as a precise micromanipulator, a tilted nanopipette was placed a few microns away from the cell surface (Fig. 5*a*). Buffer solution containing 10 μM EB was introduced in the nanopipette by applying negative potential to the internal reference electrode and then bringing the voltage to a value at which the solution flow stops (Fig. 5*b*). The pipette was slowly (0.5 μm/s) moved toward the cell and inserted into it (Fig. 5*c*). To minimize the membrane damage, the penetration depth was ≤1 μm. The applied voltage was stepped to 400 mV, at which point the aqueous solution was slowly (in ≈10 s) injected into the cell. To stop the injection, the voltage was lowered to −50 mV, so that some solution remained inside the nanopipette, and no direct contact occurred between DCE and the cell membrane (Fig. 5*d*). If a pipette is too small for videomicroscopic observation, the injection can be controlled by monitoring either syringe resistance or ion-transfer current, as discussed above. In Fig. 5, the injected volume (<100 fl) was sufficiently small, so that no changes in the cell shape, size, or position could be detected. After the complete

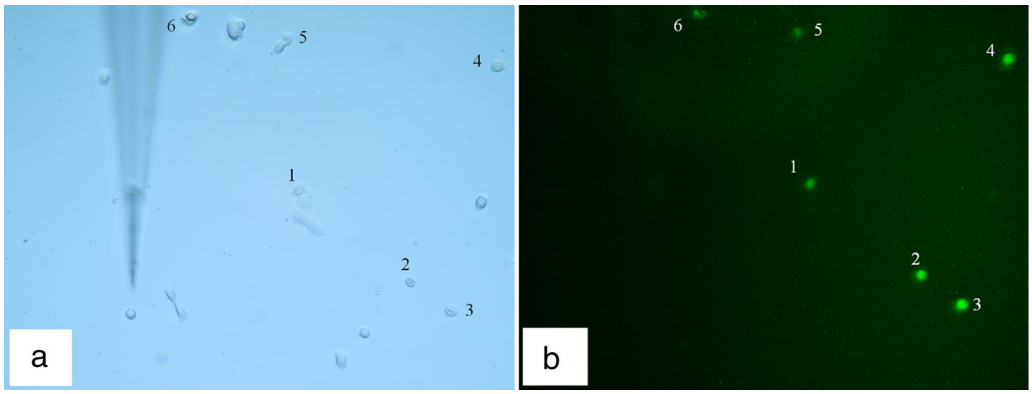

Fig. 6. Optical (*a*) and fluorescence (*b*) micrographs of immobilized MCF-10 cells. The numbers in *a* and *b* correspond to the same six cells into which BODIPY FLATP fluorescent dye was injected. (*b*) The picture was obtained ≈30 min after washing the cells with fresh buffer solution to remove excess dye.

pipette retraction, the process could be repeated to inject solution into another cell.

The insertion of the pipette into a cell shown in Fig. 5 relies on video microscopic control. Even with a relatively large orifice radius (e.g., $a = 150$ nm), the tip of the pipette is too small to be seen. With smaller pipettes, the uncertainty of positioning the pipette may become a problem. Additional control over the cell approach and penetration by the pipette can be achieved by measuring the current flowing across the liquid/liquid interface as a function of the pipette displacement. Because of the blocking effect, the current decreases sharply when the distance between the pipette tip and the cell surface becomes comparable to the pipette radius (16, 17). The current vs. pipette displacement curve can be used to estimate the tip/cell distance during the approach and subsequently control the penetration depth (*SI Text* and SI Fig. 9).

In Fig. 6, the syringe was used to inject BODIPY FLATP into immobilized MCF-10A cells. After each injection, the syringe was withdrawn and moved to the next cell. The florescence micrograph (Fig. 6*b*) shows that all cells in which the dye was injected became fluorescent. In contrast, other cells present in the optical micrograph (Fig. 6*a*) cannot be seen in Fig. 6*b* because BODIPY FLATP does not cross the cell membrane. The concentration of dye in the labeled cells did not decrease significantly with time.

Control experiments were done to verify that the solution was injected into cells by the pumping action of the syringe rather than by diffusion from the pipette or by leaking through the hole punched in the membrane. In Fig. 7, solution of EB was injected into three cells labeled with the numbers 1–3. The same pipette containing EB was used for a mock injection: the pipette was inserted in the control cell, but no solution was injected. Al-

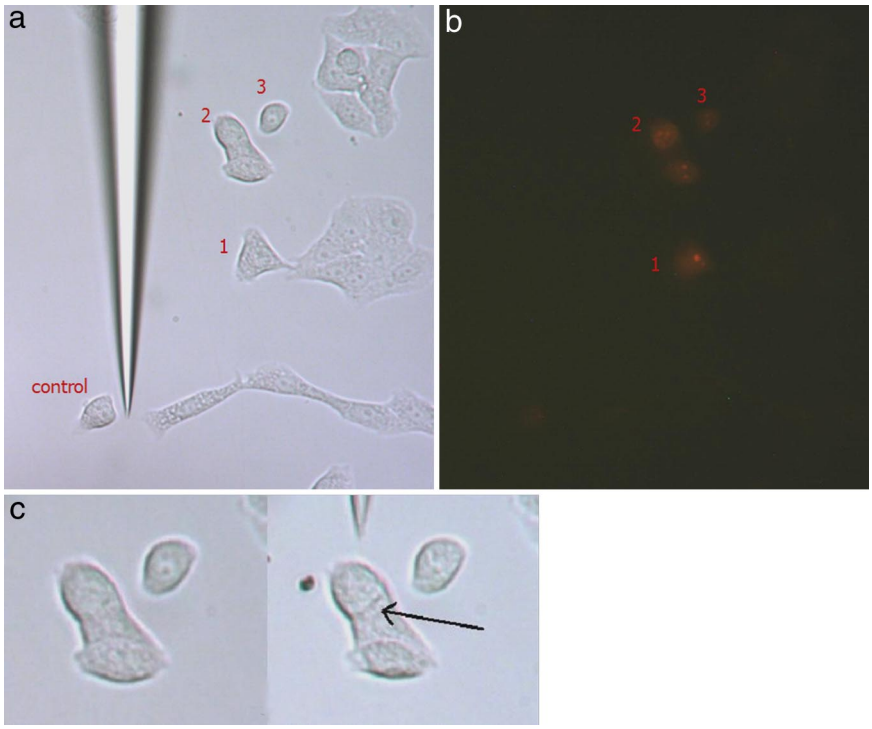

Fig. 7. Optical (*a*) and fluorescence (*b*) images of a cell field and a blown up optical micrograph of cell 2 (*c*). Cells 1, 2, and 3 were injected with a 10 μM EB buffer solution. The control cell was penetrated by the nanopipette without solution injection. (*c*) Cell 2 in the beginning of the experiment (*Left*) and ≈20 min later (*Right*). The arrow points to the membrane separation.

though the pipette spent inside the control cell approximately the same time as in each of three injected cells, the fluorescence images of these cells are markedly different: cells 1–3 have become fluorescent, but the control cell has not (Fig. 7*b*). Thus, simple diffusion of EB through the nanopipette orifice and leaking of the outer solution through the hole in the membrane are not sufficiently fast to introduce a significant amount of dye into the cell. Cell 2 in Fig. 7*b* seems to contain two stained nuclei, which resulted from a single injection of dye. The comparison of the blown up optical micrographs of the same cell in Fig. 7*c* obtained before (*Left*) and immediately after (*Right*) the injection show a line separating the two halves of the cell. This feature, which became more prominent over a few minutes time period, suggests that cell 2 was in the process of mitosis when the dye was injected.

Cell viability was verified by trypan blue-exclusion experiments. Because live cells pump out this blue dye, but dead cells do not, dead cells appear blue and live cells appear uncolored. After each series of injections, trypan blue solution ($\approx$5 μM) was added to the cell medium. In this way, all MCF-10A cells were confirmed to be alive after the injection.

Discussion

Although the basic idea of the electrochemical syringe is simple, the physicochemical processes involved in its operation are very complicated (18). The surface tension effects largely responsible for the liquid flow are not limited to the liquid/liquid interface but also depend on the water/glass and organic solvent/glass boundaries, and a three-phase water/organic/glass boundary. The properties of the inner pipette wall can be changed by modifying its surface (17, 19). Rendering the glass surface more hydrophobic, e.g., via silanization, inhibits the ingress of water into the capillary (17). In this way, both the extent of control over the solution ingress/egress and the magnitude of the required voltage can be varied.

Other parameters affecting the syringe operation include the concentrations and the nature of electrolytes in both aqueous and organic solutions. If the electrolyte concentrations are too low, the applied voltage drops within the bulk solution phase rather than across the liquid/liquid interface (10), thus preventing one from controlling the surface tension and the fluid motion. Typically, the ionic strength inside the cell and in the culture medium is sufficiently high, and the concentration of organic electrolyte should be at least 10 mM. On the other hand, by some less obvious reason, ionic concentrations that are too high either in aqueous or in organic phase (e.g., $>$0.1 M) also impair the electrochemical control of the fluid motion.

Both aqueous and organic solutions contain relatively high concentrations of ionic species, which can cross the phase boundary when voltage is applied across the liquid/liquid interface (10). For optimal syringe performance, the ion-transfer current should be minimized by using hydrophobic organic electrolyte (e.g., THATPBCl). By lowering ion-transfer current, one can also minimize the polarization of the cell membrane during the injection. Generally, the pipette current should be much smaller than the combined current through the cellular ion channels. Because an individual channel current is of the order of a few pA (20), the electrochemical injection should not cause significant depolarization of the cell membrane if the pipette current is on the pA scale.

Because the glass surface is usually charged (the charge density depends on the nature of the solution in contact with glass and its pH) (21), both electrophoresis and electroosmosis occur within the narrow shaft of the nanopipette when external voltage is applied to it (22, 23). These processes further complicate the theoretical description of the electrochemical syringe. The electrophoresis is especially important if the species to be injected into the cell are charged: whereas the injection of cationic species is facilitated by the applied voltage, anions are moved by the electric field in the opposite direction and may even be transferred to the organic filling solution. Fortunately, the expulsion of water from the pipette caused by the change in surface tension is usually faster than electrokinetic processes, and thus both cationic (e.g., EB) and anionic (e.g., BODIPY FLATP) species can be injected.

The electrochemical syringe offers several important advantages over other existing microinjectors. It is easy to fabricate, inexpensive, and easy to use. It can be made very small, and can reproducibly draw and eject small volumes of liquid as many times as needed. The electrochemical injection method does not require pressure to be applied to the nanopipette. This is an advantage because the radius of a nanopipette used for electrochemical injections can be much smaller, and a better control of the injected volume can be achieved. Unlike the stab injection method, in which the volume of injected material is determined by the time the pipette spends inside the cell, with the electrochemical syringe this time constraint is removed because the flow can be induced or stopped by changing the applied voltage. This, in turn, allows for a better control of the injection while minimizing the extent of penetration and thus reducing damage caused to the cell.

Although a small injection volume is useful when one works with biological cells, dispensing higher volumes of fluids may be required for other applications (24). With larger pipettes (e.g., $a \approx 10$ μm) that can also be used as an electrochemical syringe, one can deliver picoliter volumes of fluids. A very wide range ($\geq$6 orders of magnitude) of the dispensed solution volume suggests that electrochemical syringe can find applications in various fields from cell biology to nanolitography to microfluidics (25, 26).

Materials and Methods

Nanopipette Preparation. A Model P-2000 laser puller from Sutter Instrument (Novato, CA) was used to prepare nanopipettes from borosilicate glass capillaries (o.d. = 1 mm, i.d. = 0.58 mm), as described (11, 22). To draw/dispense aqueous solutions, a nanopipette was filled from the back with a 10 mM solution of tetrahexylammonium tetrakis(4-chlorophenyl)borate (THATPBCl) in DCE using a 10-μl syringe. To deliver organic solutions, the pipette was filled with a 100 mM aqueous $MgSO_4$. A 0.2-mm Ag wire coated with either AgTPBCl or AgCl was inserted in each pipette.

Instrumentation and Procedures. The sequences of voltage steps for egress/ingress experiments were computer-generated with the homewritten software. For the current vs. voltage measurements, a linear voltage ramp was applied to the syringe using an EI-400 bipotentiostat (Cypress Systems, Chemlsford, MA), which was also used to monitor the current flowing across the liquid/liquid interface. Experiments not involving living cells were performed in quartz cuvettes under long-distance video microscopic control (Thales Optem, Fairport, NY). The SECM instrument was homebuilt. In injection experiments, the nanopipette was attached as a probe to the 3D stage of the SECM, and the Petri dish in which a monolayer of cells was immersed in the buffer solution was mounted on the horizontal stage of an Axiovert-100 inverted fluorescence microscope (Zeiss). A video camera (IK-TU40A; Toshiba) was attached to the microscope to capture optical and fluorescence images. The SECM was set on the same optical table as the microscope so that the pipette could be positioned above the cell culture plate. A 0.2-mm Ag/AgCl electrode was immersed in the buffer solution and used as an external reference.

Cells and Reagents. Mid-passage MCF-10A cells, a human breast epithelial cell line, were cultured in DMEM/F12 media (1:1) supplemented with 5% equine serum, insulin (10 μg/ml), epi-

dermal growth factor (20 ng/ml), cholera toxin (100 ng/ml), and hydrocortisone (0.5 μg/ml) and maintained with penicillin (100 units/ml), streptomycin (100 μg/ml), and fungizone (0.5 μg/ml). Cells were redistributed at 1:3 to 1:6 every 3–4 days. Cells were plated at 5–20% confluence (2–8 $\times$ 10^3 cells per 60-mm plate) on the day before the experiment. Before each experiment, the culture medium was rinsed with a buffer containing 130 mM sucrose, 15 mM potassium chloride, 18 mM potassium acetate, 10 mM magnesium acetate, 500 μM calcium chloride, and 10 mM Hepes. All aqueous solutions were prepared from deionized water (Milli-Q; Millipore, Billerica, MA). Culture media, serum, and antibiotics (fungizone, penicillin, and streptomycin) were purchased from Invitrogen (Rockville, MD). EB from Calbiochem (San Diego, CA) was used as received. A stock solution of 10 mM EB in water was made and kept on the shelf for no more than 2 weeks. BODIPY FLATP was purchased from Invitrogen (Eugene, OR) and kept at −18°C between experiments.

Dye Injection and Imaging. The pipette tip was brought near the cell, and the medium was flushed and replaced with a sucrose buffer solution containing either EB or BODIPY FLAP fluorescent dye. The voltage applied to the syringe was stepped to −200 mV to load the nanopipette with the aqueous solution. After the desired solution volume entered the nanopipette, the voltage was changed to +400 mV to stop the ingress. Then, the voltage was raised again to +700 mV, at which point the sucrose solution was completely expelled from the syringe. This sequence was repeated several times before cell injection to verify the consistency of the syringe operation.

Using a piezo actuator of the SECM instrument, the nanopipette was moved toward the cell until its tip punctured the membrane. The voltage applied to the syringe was raised to +700 mV, at which point the sucrose solution was injected inside the cell. Care was taken not to eject all aqueous solution from the pipette to prevent the direct contact of the cell membrane with DCE. The pipette was withdrawn and moved to the next cell. The injection procedure was repeated. To obtain a fluorescence image, the medium was rinsed several times with a buffer solution containing no dye, and then a picture was taken under UV illumination.

This work was supported by National Science Foundation Grant CHE-0645958.

1. Matsuoka H, Komazaki T, Mukai Y, Shibusawa M, Akane H, Chaki A, Uetake N, Saito M (2005) *J Biotechnol* 116:185–194.
2. Felgner PL, Gadek TR, Holm M, Roman R, Chan HW, Wenz M, Northrop JP, Ringold GM, Danielsen M (1987) *Proc Natl Acad Sci USA* 84:7413–7417.
3. Neuman E, Sowers AE, Jordan CA, eds (1989) *Electroporation and Electrofusion in Cell Biology* (Plenum, New York).
4. Knoblauch M, van Bel AJE (1998) *Plant Cell* 10:35–50.
5. Laffafian I, Hallett MB (1998) *Biophys J* 75:2558–2563.
6. Knoblauch M, Hibberd J, Gray JC, van Bel AJE (1999) *Nat Biotechnol* 17:906–909.
7. Byun CK, Wang X, Pu Q, Liu S (2007) *Anal Chem* 79:3862–3866.
8. Chen X, Kis A, Zettl A, Bertozzi CR (2007) *Proc Natl Acad Sci USA* 104:8218–8222.
9. Rodolfa KT, Bruckbauer A, Zhou D, Schevchuk AI, Korchev YE, Klenerman D (2006) *Nano Lett* 6:252–257.
10. Girault HH, Schiffrin DJ (1989) in *Electroanalytical Chemistry*, ed Bard AJ (Marcel Dekker, New York), Vol 15, pp 1–141.
11. Shao Y, Mirkin MV (1997) *J Am Chem Soc* 119:8103–8104.
12. Liu B, Rotenberg SA, Mirkin MV (2000) *Proc Natl Acad Sci USA* 97:9855–9860.
13. Gabriel B, Teissié J (1998) *Bioelectrochem Bioenerg* 47:113–118.
14. Cunliffe JM, Sunahara RK, Kennedy RT (2006) *Anal Chem* 78:1731–1738.
15. Bard AJ, Mirkin MV, eds (2001) *Scanning Electrochemical Microscopy* (Marcel Dekker, New York).
16. Korchev YE, Bashford CL, Milovanovic M, Vodyanoy I, Lab MJ (1997) *Biophys J* 73:653–658.
17. Shao Y, Mirkin MV (1998) *J Phys Chem B* 102:9915–9921.
18. Mugele F, Baret JC (2005) *J Phys Condens Matter* 17:R705–R774.
19. Wang G, Zhang B, Wayment JR, Harris JM, White HS (2006) *J Am Chem Soc* 128:7679–7686.
20. Gouaux E, MacKinnon R (2005) *Science* 310:1461–1465.
21. Lavallée M, Szabo G (1969) in *Glass Microelectrodes*, eds Lavallée M, Schanne OF, Hébert NC (Wiley, New York), pp 95–110.
22. Wei C, Bard AJ, Feldberg S (1997) *Anal Chem* 69:4627–4633.
23. Keh HJ, Ma HC (2007) *Langmuir* 23:2879–2886.
24. Reichmuth DS, Shepodd TJ, Kirby B (2004) *Anal Chem* 76:5063–5068.
25. Bruckbauer A, Zhou D, Ying L, Korchev YE, Abell C, Klenerman D (2003) *J Am Chem Soc* 125:9834–9839.
26. Neugebauer S, Evans SR, Aguilar ZP, Mosbach M, Fritsch I, Schuhmann W (2004) *Anal Chem* 76:458–463.